

Article

Geocomputational Approach to Simulate and Understand the Spatial Dynamics of COVID-19 Spread in the City of Montreal, QC, Canada

Navid Mahdizadeh Gharakhanlou  and Liliana Perez * 

Laboratory of Environmental Geosimulation (LEDGE), Department of Geography, University of Montreal, 1375 Avenue Thérèse-Lavoie-Roux, Montréal, QC H2V 0B3, Canada

* Correspondence: l.perez@umontreal.ca; Tel.: +1-514-343-8003

Abstract: Throughout history, pandemics have forced societies to think beyond typical management and control protocols. The main goals of this study were to simulate and understand the spatial dynamics of COVID-19 spread and assess the efficacy of two policy measures in Montreal, Canada, to mitigate the COVID-19 outbreak. We simulated the COVID-19 outbreak using a Geographical Information System (GIS)-based agent-based model (ABM) and two management scenarios as follows: (1) human mobility reduction; and (2) observation of self-isolation. The ABM description followed the ODD (Overview, Design concepts, Details) protocol. Our simulation experiments indicated that the mainstream of COVID-19 transmissions (i.e., approximately 90.34%) occurred in public places. Besides, the results indicated that the rules aiming to reduce population mobility, led to a reduction of about 63 infected people each week, on average. Furthermore, our scenarios revealed that if instead of 42% (i.e., the adjusted value in the calibration), 10%, 20%, and 30% of infectious people had followed the self-isolation measure, the number of infected people would have risen by approximately 259, 207, and 83 more each week, on average, respectively. The map of critical locations of COVID-19 spreading resulted from our modeling and the evaluated effectiveness of two control measures on the COVID-19 outbreak could assist health policymakers to navigate through the pandemic.

Keywords: COVID-19; geographical information system (GIS); complex system (CS); agent-based modeling (ABM) approach; epidemic dynamics; epidemic outbreaks; Canada



Citation: Mahdizadeh Gharakhanlou, N.; Perez, L. Geocomputational Approach to Simulate and Understand the Spatial Dynamics of COVID-19 Spread in the City of Montreal, QC, Canada. *ISPRS Int. J. Geo-Inf.* **2022**, *11*, 596. <https://doi.org/10.3390/ijgi11120596>

Academic Editors: Wolfgang Kainz, Fazlay S. Faruque, Peng Jia and Mo Ashifur Rahim

Received: 14 October 2022

Accepted: 24 November 2022

Published: 27 November 2022

Publisher's Note: MDPI stays neutral with regard to jurisdictional claims in published maps and institutional affiliations.



Copyright: © 2022 by the authors. Licensee MDPI, Basel, Switzerland. This article is an open access article distributed under the terms and conditions of the Creative Commons Attribution (CC BY) license (<https://creativecommons.org/licenses/by/4.0/>).

1. Introduction

The emergence and initial outbreak of the novel Coronavirus (i.e., COVID-19) from Wuhan, China, in 2019 has become a global health concern [1]. Among the pandemic diseases that humans have faced in the twenty-first century (e.g., H1N1, Polio, Zika, Ebola, etc.), none have had a global public health burden as COVID-19 [2].

Combating the COVID-19 pandemic and offering insightful information for health policymakers can be aided by monitoring the dynamic spread of the disease, the concentration of disease cases, and identifying potential hotspots of infections [3–5]. Numerous studies have pointed out the Geographical Information System (GIS) as an essential tool to analyze the spatial distribution of infectious diseases, identify the pandemic path, and determine the hotspots of the disease spread [3,4,6]. However, relying just on spatial data and GIS analyses is insufficient to account for the dynamics and complexity of disease spread.

The rising impacts of the COVID-19 epidemic have made urgent COVID-19 research necessary, while at the same time, the inevitability of framing human systems as complex systems has attracted the interest and attention of researchers [7,8]. Many natural and artificial systems exhibit seemingly complex behaviors because of dense nonlinear spatiotemporal interactions among many autonomous component systems at various levels of an organization. Complex Systems is a term coined to describe these systems and are at the heart of many of today's issues [9]. One of the most remarkable features of complex systems

is considering the local interactions between self-organizing components that give rise to the emergence of novel global patterns [10]. This hallmark of complex systems is overlooked in traditional epidemiological models, particularly mathematical models [11,12]. Cellular automata (CA) and agent-based modeling (ABM) are two main complex systems modeling approaches. The CA modeling approach consists of a grid of cells, each of which is in one of a finite number of statuses so that statuses vary based on a set of rules passing among adjacent cells [13,14]. The ABM, as another robust complex systems modeling approach, is composed of autonomous interacting individuals (i.e., agents) with attributes and behaviors [15,16]. This modeling approach considers various behaviors for agents and attempts to model dynamic and complex phenomena by considering interactions between agents as well as agents and the environment [15,16].

In the simulation of epidemiologic disease spread, both ABM and CA modeling approaches have been extensively suggested and employed [17–20]. The capability of ABM in taking into account (1) the heterogeneous individuals and the environment; (2) the dynamic movements of individuals; (3) the interactions between individuals as well as individuals and the environment; (4) the characteristics of individuals, the environment, as well as the biological and epidemiological characteristics of the disease; and (5) a range of possible “what if” scenarios make the ABM approach much flexible, useful, and realistic in simulating epidemiologic disease outbreaks [20,21].

As of the emergence of COVID-19, simulation of the COVID-19 outbreaks, and the significant adeptness of COVID-19 control measures using the ABM approach have been highlighted in earlier studies [7,22–29]. The only study that employed the ABM approach to simulate the COVID-19 spread in Montreal was the study by Manout and Ciari (2021) [30]. In their study, the relationship between everyday activities, their spatial and temporal distribution, the attributes of the individuals, and the infection spread were evaluated. The findings of their study highlighted the substantial contribution that activities associated to the home, workplace, and schools have in the spread of disease.

The main purposes of this study were to develop a spatially explicit agent-based model to simulate the dynamics of COVID-19 spread and assess the effectiveness of two control interventions in containing the COVID-19 outbreak in the city of Montreal, QC, Canada. Besides these purposes, the motivations of this study were investigated to address the following research concerns: (1) how could the epidemiological modeling approach take into account the dynamics of the disease spread in relation to the spatial data?; (2) how is the infection spread through a population?; (3) which age groups are most frequently exposed to the infection transmission?, and finally; (4) which areas of Montreal are the main spots for COVID-19 transmission? The specific highlight of the presented study that differentiated it from preceding ones was its ability to address these concerns by developing a spatially explicit agent-based model.

2. Materials and Methods

2.1. Overview of the Area under Study

As of the start of COVID-19 outbreak in Canada (i.e., 25 January 2020), various control interventions (e.g., educational places closures, restriction in people movements, heeding physical distancing, self-isolation on symptoms, etc.) were employed to contain the spread of the virus. Nevertheless, the epidemic continued to hit the country on 21 January 2021. Among the Canadian provinces, Quebec had the highest number of confirmed cases, and Montreal with 39.1% of total confirmed cases, was the city with the highest number of confirmed cases in the province of Quebec; consequently, this study was carried out in the city of Montreal.

2.2. Data and Preprocessing of the Input Data

Having reviewed studies to identify the data required in simulating the COVID-19 outbreak, the essential data were collected and processed. These data included land-use, demographic information of Montreal (e.g., population (Table A1), number of total house-

holds, and household size (Table A2)), labor statistics (Table A3), information about the control interventions employed in Montreal since the COVID-19 pandemic, and finally daily confirmed cases of COVID-19 in Montreal during the simulation period. The preparation process of data was performed once all the required data were collected. In doing so, land use data were stratified into four major groups: residential places, workplaces, educational places, and the rest of the places labeled “public places” (e.g., parks, agriculture places, religious places, etc.) (Figure 1A). Besides, the population density map (Figure 1B) was used in the distribution of human agents.

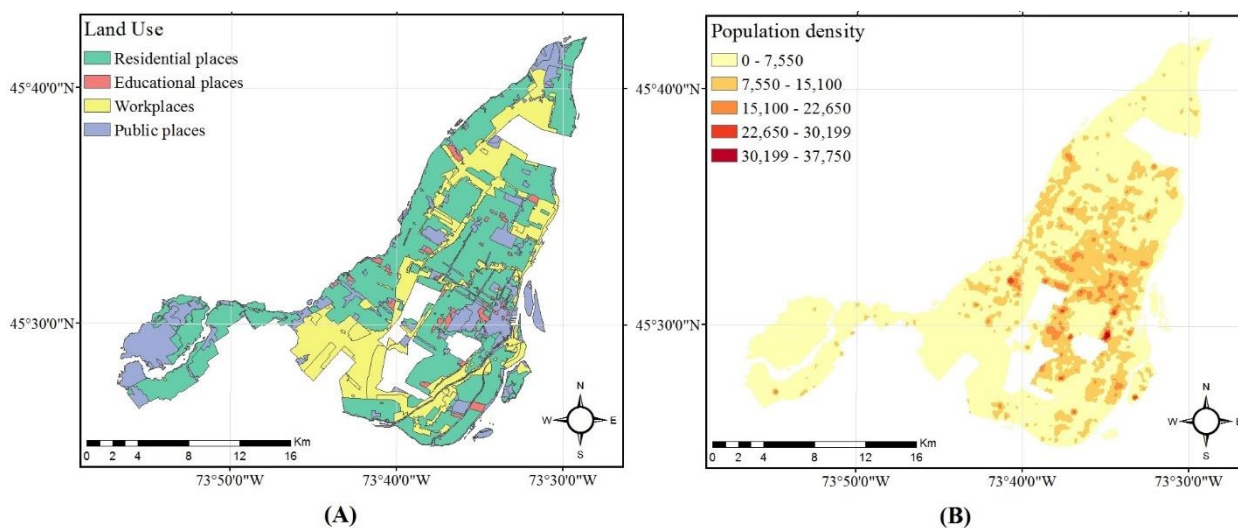


Figure 1. (A) The land use of Montreal in four groups; and (B) the population density of Montreal.

2.3. The Proposed Agent-Based Model

The simulation of the COVID-19 outbreak in this study was implemented in Mesa framework (i.e., an ABM framework in Python) [31,32]. The flowchart of code implementation on the Mesa framework was clearly illustrated in Figure A1. To describe the proposed agent-based model in a way more understandable and comprehensive, the ODD (Overview, Design concepts, Details) protocol was used [33,34]. The remainder of this section contains a detailed explanation of each ODD protocol component for this study.

2.3.1. Model Overview

This element of the ODD protocol lies in three sub-elements including (i) a summary but much detailed description of a model’s purpose (see Section Purpose); (ii) the model’s entities, their state variables (possibly including behavioral attributes and model parameters), and the model’s spatial and temporal scales (see Section State Variables and Scales); and (iii) a detailed and precise description of the model’s schedule in sequential order (see Section Process Overview and Scheduling).

Purpose

The main purposes of the proposed model were to simulate the COVID-19 outbreak and assess the effectiveness of control strategies. The essential causes of the COVID-19 outbreak are the movement of humans and their interactions with each other [22]. Accordingly, developing a realistic dynamic model that considers the interactions and movements of people is critical for assessing the COVID-19 epidemic, and we included them in our model.

State Variables and Scales

The constructing components of our model involved human agents and the geographic environment which abstractly represented the study area. To represent the components,

a unified modeling language (UML) class diagram was used (Figure 2). Regarding the UML class diagram, the environment of the model was constructed according to several spatial data. Various attributes were assigned to the cells whose attributes were correspondingly initialized based on the spatial data. Besides, several attributes and behaviors were taken into consideration for the human agents. All explained details were schematically illustrated in Figure 2.

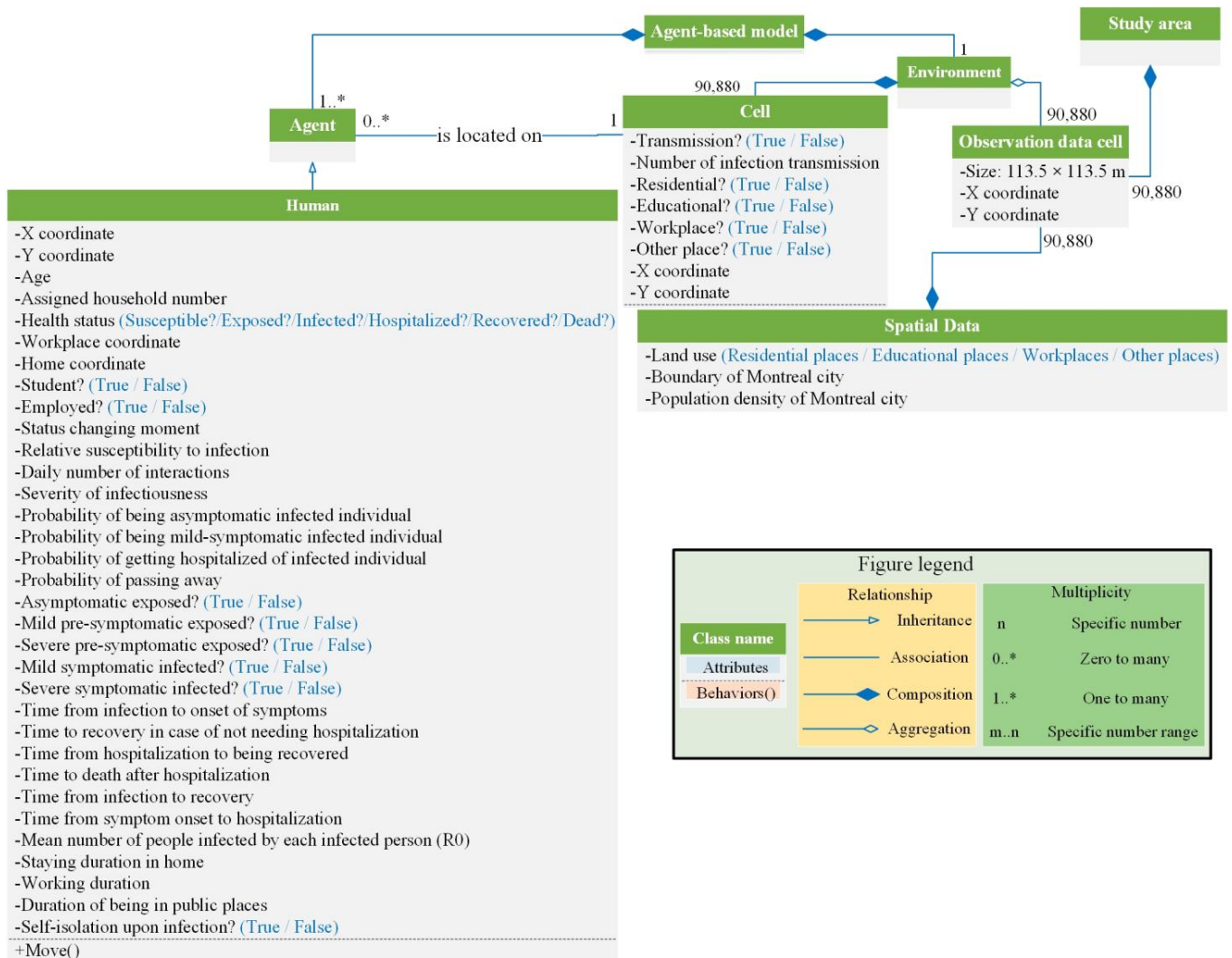


Figure 2. Representation of the components of the proposed model.

The framework included the landscape of Montreal on which human agents interact and move. The landscape of Montreal was divided into a 320×284 grid with a cell size of 113.5 m due to the spatial resolution of data. Besides, the simulation step was set to one hour and the model was run for 5 weeks.

Process Overview and Scheduling

An outline of sequences of the processes that are carried out during the simulation is given in this element of the ODD protocol. In the first step, all spatial data were loaded. Next, for each spatial data, an attribute was defined for the cells and their values were correspondingly initialized regarding the spatial data. In the third step, human agents were created in the number of the population and concerning the demographic conditions of the city. Human agents randomly but based on the population density map were distributed as groups (i.e., households) in the residential cells of the environment. Moreover,

a vast number of attributes were born in mind for human agents and their attributes were initialized based on information such as the biological and epidemiological characteristics of COVID-19 disease, demographic conditions of Montreal, etc. These steps were done only once and at the beginning of the model. The dynamic and iterative processes of the model began performing once the first three major steps were completed. The main dynamic processes of the proposed agent-based model involved: (1) the hourly location of human agents; (2) the interaction level of human agents based on their current locations; (3) the dynamics of the control interventions employed along with their various influences on human agents' movement as well as their interactions in the environment; and (4) the epidemic process and transition of human agents from different health statuses.

2.3.2. Design Concepts

In this element of the ODD protocol, the way that simple fundamental principles addressed in the design of a more realistic and complex model is explained. In this element of the ODD protocol, some necessary design concepts of the proposed agent-based model including sensing (see Section Sensing), interactions (see Section Interactions), and stochasticity (see Section Stochasticity) are described.

Sensing

In the model, the human agents had the sense to identify the cells for moving in the environment. Human agents were able to identify their workplace, public place, and residential cells. They were also capable of sensing other human agents in the same cell as themselves. Furthermore, human agents began or stopped doing certain of the tasks depending on whether a control measure was employed.

Interactions

The COVID-19 disease spreads because of human agents interacting with one another. Accordingly, the proposed model included the interactions between human agents as well as between human agents and the environment. Human agents by interacting with the environment were choosing the cells to move over time steps. Besides, an increase in the number of infection transmission in cells was happening when the infection transmission was being taken place in the cells. Furthermore, human agents interacted with each other, and their interaction level varied based on their current location.

Stochasticity

Several stochastic processes were considered within our model to present natural processes. For instance, choosing the workplace cell for human agents included stochasticity. Although selecting a residential cell for human agents was performed regarding the population density and the Roulette wheel selection method, it was probabilistic. Randomly assigning human agents to the households, choosing public places by human agents to move, and initializing some of the human agents' attributes all were other stochastic processes considered in our model.

2.3.3. Details

In this element, the further details of the model and the implementation of the model are explicitly and comprehensively described. Regarding this element of the ODD protocol, model details and the implementation process of the model are performed in several sections: initialization (see Section Initialization), input data (see Section Input Data), and submodels (see Section Submodels).

Initialization

In this section, the values of the state variables at the beginning of the model were initialized. Besides, change or no change in values of the variables were clarified and provided in accordance with reliable references. In the beginning, the data related to the

landscape information of the study area were uploaded and initial values of the cells' attributes were set. Besides, a specific number of agents regarding the population data were created and their attributes were initialized regarding the reliable official data sources and the previous studies. All the parameters were summarized in Table 1.

Table 1. Summary of the input parameters.

Parameters	Symbol	Value/Range of Value	Mean (μ)	Standard Deviation (σ)	Resources
Time from infection to onset of symptoms	τ_{sym}	Gamma (k, θ); $k = \mu^2 / \sigma^2, \theta = \sigma^2 / \mu$	5.42 days	2.7 days	McAloon et al., 2020 [35]
Time to recover in case of not needing hospitalization	τ_{rec}	Gamma (k, θ); $k = \mu^2 / \sigma^2, \theta = \sigma^2 / \mu$	12 days	5 days	
Time from hospitalization to being recovered	$\tau_{hosp, rec}$	Gamma (k, θ); $k = \mu^2 / \sigma^2, \theta = \sigma^2 / \mu$	8.75 days	8.75 days	Hinch et al., 2021 [36]
Time to death after hospitalization	τ_{death}	Gamma (k, θ); $k = \mu^2 / \sigma^2, \theta = \sigma^2 / \mu$	11.74 days	8.79 days	
Time from infection to recovery (for asymptomatic individuals)	$\tau_{a, rec}$	Gamma (k, θ); $k = \mu^2 / \sigma^2, \theta = \sigma^2 / \mu$	15 days	5 days	
Time from symptom onset to hospitalization	τ_{hosp}	Gamma (k, θ); $k = \mu^2 / \sigma^2, \theta = \sigma^2 / \mu$	5.14 days	4.2 days	Pellis et al., 2020 [37]
Mean number of people infected by each infectious person	R_0	(3.66–5.58)	4.5 people	(4.5/8) people	Ke et al., 2021 [38]
The fraction of asymptomatic infected individuals	$\Phi_{asym}(age)$	Age	Value	-	-
		0–9	0.456		
		10–19	0.412		
		20–29	0.370		
		30–39	0.332		
		40–49	0.296		
		50–59	0.265		
		60–69	0.238		
70+	0.214				
centering The fraction of infected individuals with mild symptoms	centering $\Phi_{mild}(age)$	0–9	0.533	-	-
		10–19	0.569		
		20–29	0.597		
		30–39	0.614		
		40–49	0.616		
		50–59	0.602		
		60–69	0.571		
		70+	0.523		
					Riccardo et al., 2020 [39]

Table 1. Cont.

Parameters	Symbol	Value/Range of Value	Mean (μ)	Standard Deviation (σ)	Resources
The fraction of infected individuals with severe symptoms who are hospitalized	$\Phi_{hosp}(age)$	0–9	0.001	-	-
		10–19	0.006		
		20–29	0.015		
		30–39	0.069		
		40–49	0.219		
		50–59	0.279		
		60–69	0.370		
		70+	0.391		
The fraction of fatalities amongst individuals with severe symptoms who are hospitalized	$\Phi_{death}(age)$	0–9	0.33	-	-
		10–19	0.25		
		20–29	0.5		
		30–39	0.5		
		40–49	0.5		
		50–59	0.69		
		60–69	0.65		
		70+	0.88		

Input Data

All the input data and the preparing processes of input data were explicitly described in Section 2.2. Having performed the preprocessing of the input data and converted them to ASCII format, they were imported into the Mesa framework [31,32]. Table 2 listed all the model's input data along with their sources.

Table 2. Summary of the input data.

Data		Source
Spatial data (Vector)	The boundary of Montreal city	These data were obtained from this web page: https://donnees.montreal.ca/ (accessed on 23 March 2022).
	Land use	
Polygon	Montreal city-dwelling counts by dissemination area	Canadian Population & Dwelling Counts by Dissemination Area, 2016; the data were obtained from this web page: https://resources-covid19canada.hub.arcgis.com/datasets/esrica-tsg::canadian-population-dwelling-counts-by-dissemination-area-2016 (accessed on 23 March 2022).
Demographic information of Montreal city		Statistics Canada, Census of Population 2016; the data were obtained from this web page: https://www12.statcan.gc.ca/census-recensement/2016/dp-pd/index-fra.cfm (accessed on 23 March 2022).
Human mobility reduction due to the COVID-19		The data were obtained from this web page: https://www.google.com/covid19/mobility/ (accessed on 24 April 2022).
Weekly confirmed cases of COVID-19 in Montreal		The data were obtained from this web page: https://santemontreal.qc.ca/en/public/coronavirus-covid-19/situation-of-the-coronavirus-covid-19-in-montreal/#c46934 (accessed on 24 April 2022).

Submodels

There are some detailed aspects of the proposed model that were explicitly explained in the remainder of this section.

The Spatially Xplicit Environment

Concerning the uneven distribution of population and the unequal spread of COVID-19 over a region, it is evident that geography and space have a significant impact on the COVID-19 epidemic [7,23,41,42]. Furthermore, COVID-19 is a dynamic phenomenon that is highly dependent on people’s interactions and mobility [43]. People’s interactions and mobility are both geographically related and change from place to place [22]. Accordingly, the environment of the model was designed with all the spatial data relevant to the COVID-19 outbreak.

Agents

In this study, each human agent was considered as a representative of 100 people in the real world. Each human agent was assigned to a specific household and the households were formed according to the household’s size. Rather than being distributed individually, human agents were distributed in the context of the household. The distribution of households was done regarding the population density map and the Roulette Wheel method. Besides, human agents, in terms of occupation, were stratified into three main groups including student, employed, and unemployed in response to Montreal labor statistics (Table A3).

After that human agents were created and distributed in the environment, the movement of human agents and their interactions with each other were implemented. The locations of human agents were considered variant on an hourly basis. In this study, an hourly activity was allocated to human agents such that they were intended to move throughout the environment according to these hourly tasks (Figure 3). It is worth mentioning that the hourly activity of human agents was simulated in consideration of both, the land use characteristic of the environment and the attributes of human agents (such as age and occupation).

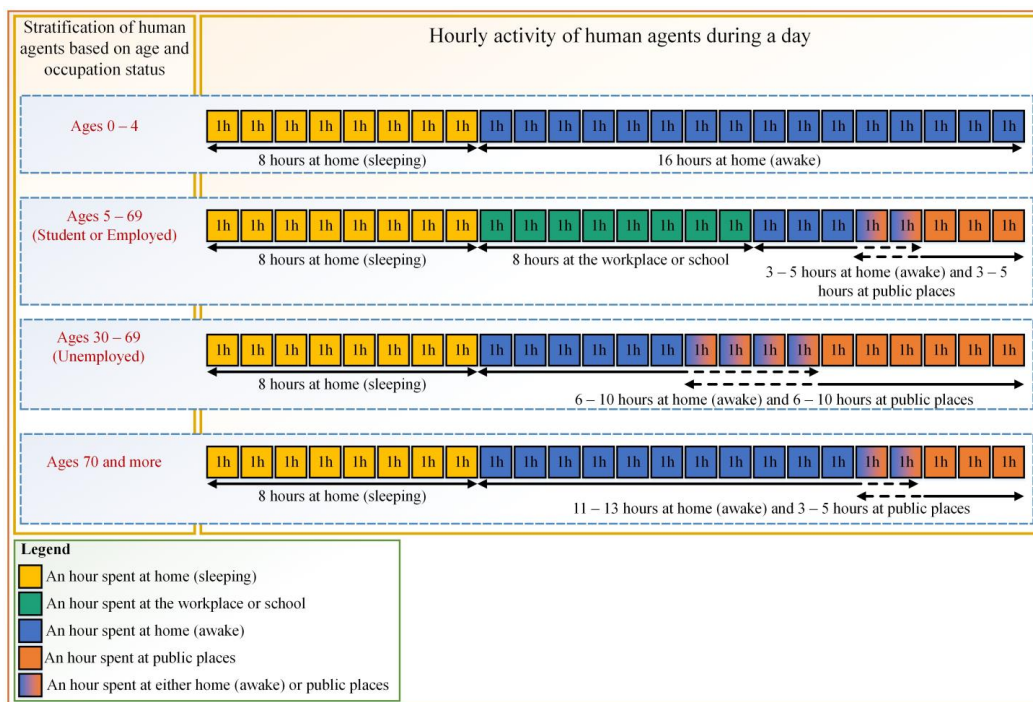


Figure 3. The hourly activity of human agents during a day based on their age and occupation.

Depending on where human agents were, their interactions fluctuated on two different levels: (1) when they were at residential places; and (2) when they were at workplaces or public places. Human agents have the highest level of interaction when they are at their residential places so that based on their interaction level, the transmission of the disease was considered variable.

The Epidemiological Submodel

Concerning people’s status progressing in COVID-19 disease, human agents at any moment in the model were only in one of the statuses of susceptible, exposed, infectious, recovered, hospitalized, or dead, and based on the events that were happening during the simulation, their statuses continuously changed over time. The vaccinated status was not considered for the human agents in the model because the vaccination procedure began in Montreal on 1 March 2021. Figure 4 explicitly elucidated numerous human agent statuses, the transition of human agents from one status to another, the period of transition (T_{xxx}), and the probability of being placed in a specific status based on their age ($\Phi_{xxx}(age)$).

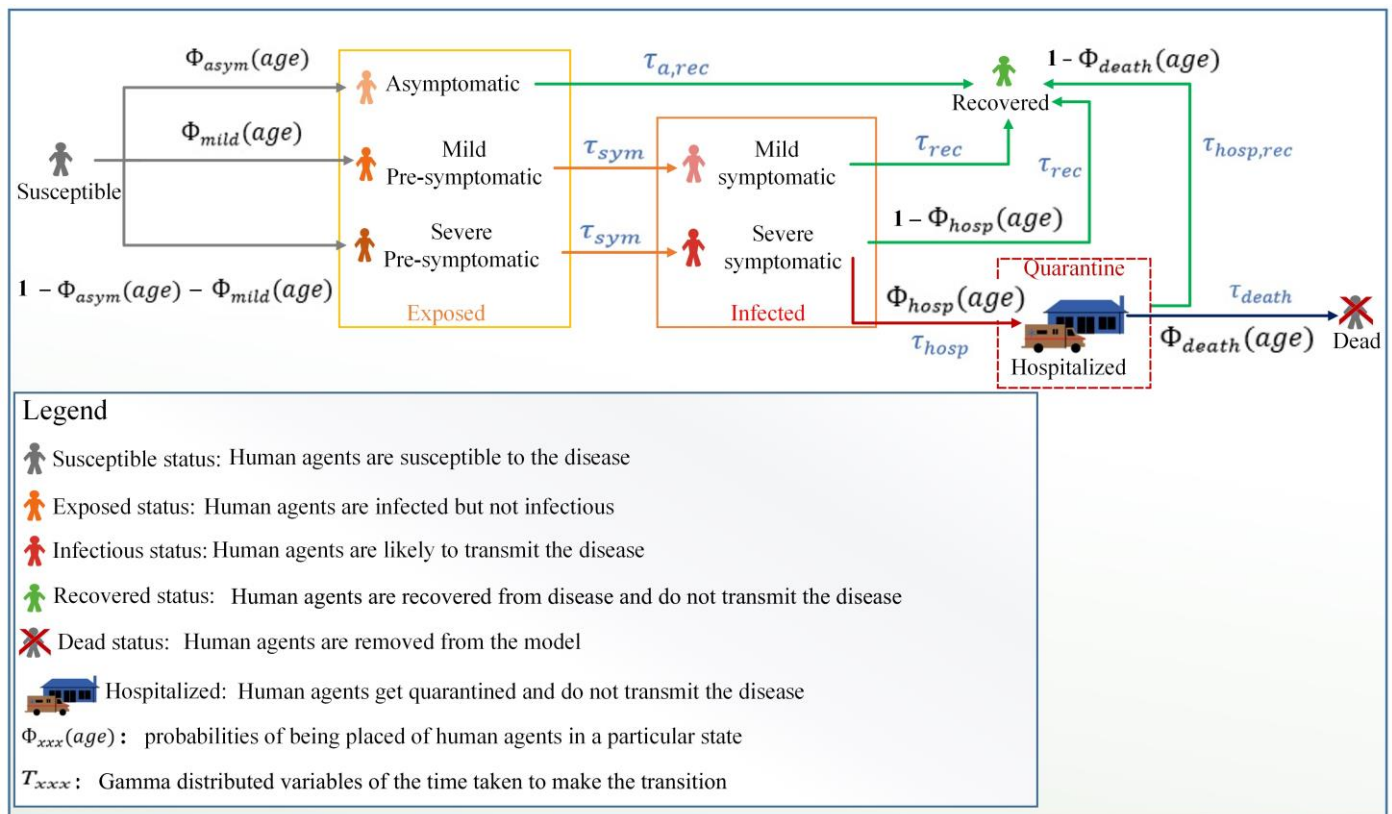


Figure 4. The probability and time distribution of transitions, and the health status of human agents.

The infection was assumed to transmit from those who were infectious (i.e., source) to ones who were susceptible to infection (i.e., recipient) in case of interaction with each other. The rate of infection transmission was considered dependent on three factors: (1) the recipient’s susceptibility depending on age; (2) the source’s infectiousness severity; and (3) the interaction level between source and recipient agents.

To calculate the infection transmission probability (P), first, the hazard rate per interaction (λ) was calculated according to Equation (1). After calculating the hazard rate, the probability of infection transmission was calculated regarding Equation (2) [36].

$$\lambda(t, v, a, n) = \frac{R_0 S_a n A_d}{\bar{I}} \int_t^v f_{\Gamma}(u; \mu_i, \sigma_i^2) du \tag{1}$$

$$P = 1 - e^{-\lambda} \quad (2)$$

Here, t and v are the beginning and the current time of infection, respectively; a is the age of the recipient; n is the type of interaction; R_0 is the mean number of people infected by each infectious person; S_a is the relative susceptibility of the recipient; A_d is the relative infectiousness of the source; I is the mean number of daily interactions; f_Γ is the probability density function of a gamma distribution; and finally, μ_i and σ_i , respectively, are the mean and standard deviation of the infectiousness curve. The parameters along with their values were summarized in Table A4.

Due to the closeness of interactions in the household compared to the other two types, the parameter n was given the value of two for those occurring within the household, while its value for the other two types was given the value of one [36]. Owing to the strong age structure of the COVID-19 progression, the susceptibility of the recipient was considered dependent on age. Besides, the infectiousness of infected individuals with no symptoms and mild symptoms was 0.33 and 0.72 times that of those with severe symptoms, respectively [36]. Additionally, following Mossong et al., 2008 [44], the value for the number of daily interactions was derived using a normal distribution and assigned to human agents with regard to their age (Table A5).

Control Interventions

Given that the closure of educational centers intervention had been employed in Montreal as of the COVID-19 outbreak, this intervention was assumed in our model at the outset. Besides, two other crucial yet underappreciated control interventions were considered, and their efficacy was investigated. The functionality of the control interventions was explicitly described in this section.

Reduction in human movements: the outbreak of COVID-19 desists in the unmitigated absence of people's movements; so, one of the factors playing a significant role in the COVID-19 outbreak is people mobility. To consider this intervention in the model, the fraction of human agents' movement to the specific places was reduced regarding the land use of the places as well as the occupation of the human agents.

Self-isolation upon symptoms: self-isolation refers to the separation of infectious people from the rest of the people to protect non-infected people (i.e., the infectious people get quarantined). Following this intervention, infectious people stop moving as well as interacting with others; accordingly, this intervention might end up greatly reducing the number of infected people. To apply the self-isolation intervention in the model, the movements and interactions of infectious human agents were completely restricted in the model.

2.3.4. Verification Process

The first step prior to interpreting the results of the model is making sure of its consistency with its design concepts (i.e., verification process) [45]. To do so, two arbitrary scenarios were designed, and the verification of the model was evaluated in each scenario by maintaining all parameters constant and changing only one parameter. The number of infectious human agents at the beginning of the simulation and the reduction in human agents' movement to the public places were altered in the first and second scenarios, respectively, while the other parameters were left unchanged.

2.3.5. Calibration and Validation

Calibration and validation are ongoing challenges in the ABM approach. Calibration entails running the model with various parameters and comparing the output to empirical data to find parameter settings that minimize the model's error. There are two main quantitative calibration approaches for ABMs: (1) point estimation; and (2) categorical or distributional estimation [46]. While the point estimation approach seeks out a single parameter combination that provides the best fit to data, the categorical estimation approach assigns a probability to numerous parameter possibilities across a range of reasonable

values [47]. Besides, the categorical calibration approach has the benefit of providing supplementary information on parameter uncertainty as well as the uncertainty of the model's results. Amongst various categorical calibration methods, we used the history matching (HM) method to calibrate our model due to its ability in considering uncertainties of the model and observations [48]. The methodology of the HM method was presented in Figure 5.

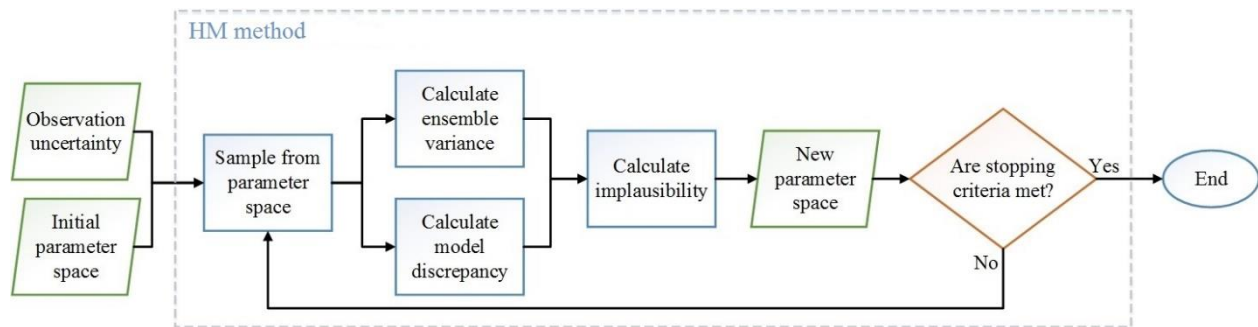


Figure 5. The functionality of the HM method used for model calibration.

The unknown parameters in our model were: the number of exposed and infectious cases at the beginning of the simulation (i.e., the date 5 January 2021, was considered as the beginning of the simulation) as well as the unknown percentage of people who isolated themselves (i.e., get quarantined) upon transition to infectious status. The number of newly infected human agents on a weekly basis was considered as the output of the model. Since the model's unknown parameters were either percentages or positive integers, the potential ranges for each parameter (i.e., the parameter space) were determined to be between 0 and 1 for percentages and larger than zero for the remaining parameters. Since the unknown parameters' spaces were large and continuous, the Latin-Hypercube Sampling (LHS) method was used to pick samples to run the HM method on the parameter space [48].

The uncertainties in our model were estimated by exploring the parameter space of a model by picking a subset of the samples from different clusters. Having run the model once for each sample, the variance of the errors across samples was determined according to Equation (3). Besides, the observations' uncertainty was set to zero since there were no direct means to measure them several times and calculate the variance.

$$V_m^r = \frac{1}{N-1} \sum_{n=1}^N (d(z^r, f^r(x_n)) - E^r(x))^2 \quad (3)$$

Here, N is the total number of samples used, d is the error between the r^{th} expected output (z^r) and r^{th} model output $f^r(x_n)$ for the parameters x_n , and $E^r(x)$ is the average model error for each parameter set in x .

To determine the ensemble variance (i.e., the uncertainty in models due to the stochastic processes), the model was run K times on a subset of N samples, and the variance was estimated between the K runs, as well as the average variance over the N samples, using Equation (4) and auxiliary Equation (5).

$$V_s^r = \frac{1}{N} \sum_{n=1}^N \left[\frac{1}{K-1} \sum_{k=1}^K (d(z^r, f^r(x_n)) - E_K^r(x_n))^2 \right] \quad (4)$$

$$E_K^r(x_n) = \frac{1}{K} \sum_{k=1}^K d(z^r, f^r(x_n)) \quad (5)$$

Here, V_s^r is the ensemble variance, K is the total number of runs in an ensemble, $f^r(x_n)$ is the r^{th} output from the k^{th} run of the model with parameters x_n , and $E^r(x_n)$ is the average model error across the ensembles.

To calculate the implausibility of a set of inputs and investigate their eligibility, the model output was compared to the expected output assuming observations' uncertainty equals zero Equation (6).

$$I^r(x) = \frac{(z^r - f^r(x_n))^2}{V_s^r + V_m^r} \quad (6)$$

Regarding the implausibility value (i.e., $I^r(x)$), we considered a constant threshold, indicated c , to assess whether x is implausible. If $I^r(x) \geq c$, the difference between predicted and expected output was regarded as too large. Otherwise, x was included in the non-implausible space. Pukelsheim's 3σ rule was used to determine the threshold of c [49]. This means that with a chance of at least 0.95, the proper selection of parameters x will result in $I^r(x) < 3$. The HM procedure was kept carrying out until the stopping conditions were reached. In our situation, the stopping criteria were fulfilled when either all the parameters were found to be non-implausible, or the non-implausible space did not diminish.

To evaluate the closeness of two sets of predicted and actual observed values (i.e., validation process), the Chi-square test was utilized. Deciding to either reject or accept the null hypothesis (i.e., the predicted values are close enough to the actual observed values) is performed regarding the Chi-square statistic (Equation (7)).

$$\chi^2 = \sum_{q=1}^m \frac{(P_k - O_k)^2}{O_k} \quad (7)$$

Here, P_k and O_k are the averages of newly infected human agents on a weekly basis in 30 runs and associated weekly confirmed cases, respectively; the suffix q runs over weeks, and m is the number of weeks (i.e., $m = 5$). To determine statistical significance, we compared the values at the 5% significance level.

3. Results

3.1. Model Verification

In the first scenario, we evaluated 10, 20, and 40 infectious human agents and compared the average number of newly infected human agents derived after 30 runs. After 30 runs, the average number of newly infected human agents rose as expected by increasing the number of infectious human agents at the beginning of the simulation while maintaining the remaining parameters constant, as follows: 126.63, 181.47, and 344.13 for 10, 20, and 40 infectious human agents, respectively. It is worth mentioning that the number of exposed human agents, the value of the self-isolation parameter, and the percentage of reduction in humans' movement to public places and workplaces were 10, 10%, 33%, and 18%, respectively.

In the second scenario, we considered three different reductions in human mobility to public places: 10%, 30%, and 50%. For each of these three settings, the model was run 30 times, and the average numbers of newly infected human agents were compared. Reducing humans' movement, as expected, would result in a reduction in the number of infected human agents in the model. The average number of newly infected human agents was 180.73, 106.27, and 76.83 for 10%, 30%, and 50%, respectively. It is worth noting that the number of exposed human agents, the number of infectious human agents, the value of the self-isolation parameter, and the percentage of reduction in humans' movement to workplaces were 10, 10, 10%, and 18%, respectively. Regarding two scenarios, it was confirmed that the proposed agent-based model accurately represented the conceptual description and specifications.

3.2. Model Calibration and Validation

Adjusting values for unknown parameters at the initial condition of the model was performed using the HM method. The proposed model was calibrated when the value of 1, 3, and 42% were assigned to the number of exposed human agents, the number of infectious human agents, and the percentage of people isolating themselves upon transition to infectious status, respectively.

Irrespective of assuming the observations' uncertainty equals zero due to the lack of direct means to measure them several times, disease statistics contain various sources of error [50]. Accordingly, to reduce the impact of observations' uncertainty on the model, the model's outputs were evaluated based on the weekly cases.

Having adjusted the values found for the unknown parameters in the calibration procedure, the proposed model was validated using the Chi-square test. χ^2 yielded the value of 9.2879, which in comparison to the critical value (i.e., $X_{0.05}^2(4) = 9.488$) was lower and demonstrated the acceptance of the null hypothesis. In other words, the Chi-square test indicated that the results of our model were close enough to actual observed values.

3.3. Model Outputs

In addition to tracking the weekly averages of newly infected human agents, to trace the disease outbreak over time as well as achieve additional information on disease outbreak, the momentum number of human agents in each status over the simulation was depicted in Figure 6. Besides, infected human agents were tracked regarding their age (Figure 7); and finally, the places in which the COVID-19 transmission occurred were ascertained and elucidated in Figure 8. It is worth mentioning that having obtained the outputs of the agent-based model (i.e., the frequency and locations of weekly infection transmission) in thirty runs, they were imported into the ArcGIS software and the Raster Calculator tool was used to calculate the average of thirty outputs of the agent-based model (i.e., the average frequency of weekly infection transmission). Following these outputs, the spatial and temporal patterns of the COVID-19 outbreak can be traced.

Concerning Figure 7, the majority of infected human agents were beyond the age of 20. Furthermore, given the comparison of the model's results (Figure 8) and the land use map (Figure 1A), it was inferred that the majority of COVID-19 transmission (i.e., approximately 90.34%) occurred in public places. Besides, about 6.76% and 2.9% of COVID-19 transmission took place in residential places and workplaces, respectively.

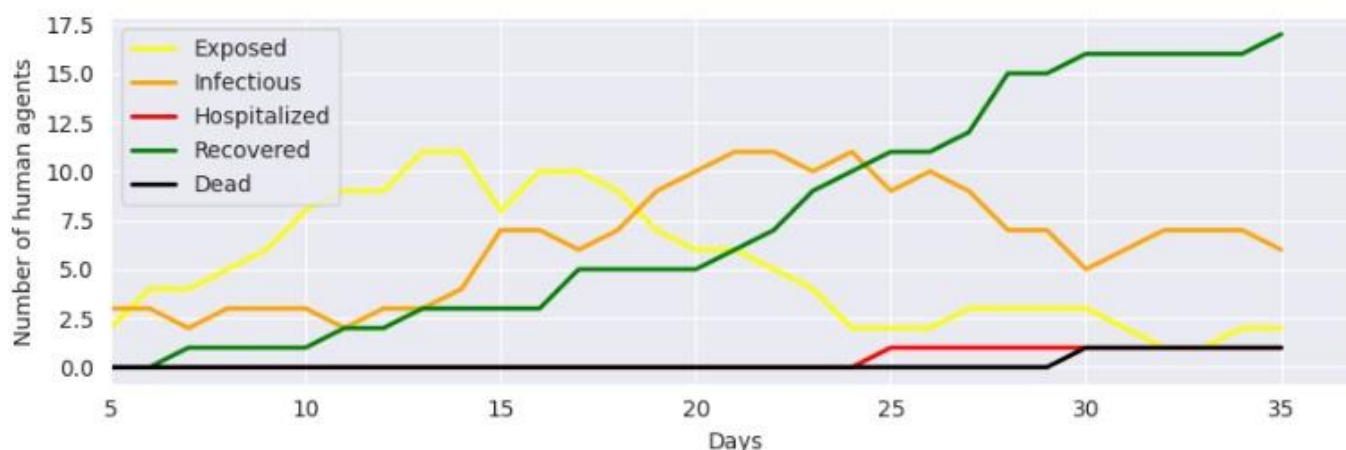


Figure 6. The momentum number of human agents in each status over the simulation (the result of an example run); each agent is a representative of 100 people.

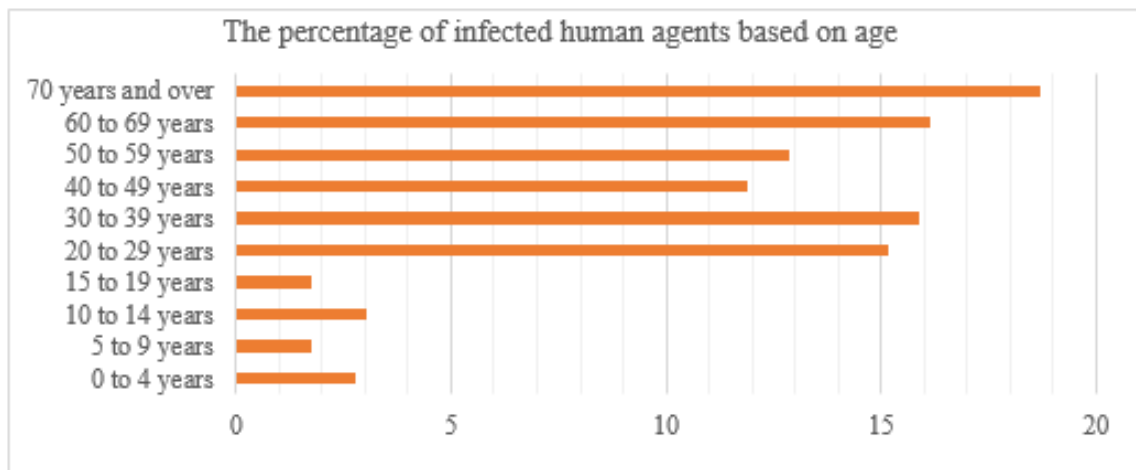


Figure 7. The percentage of infected human agents based on age.

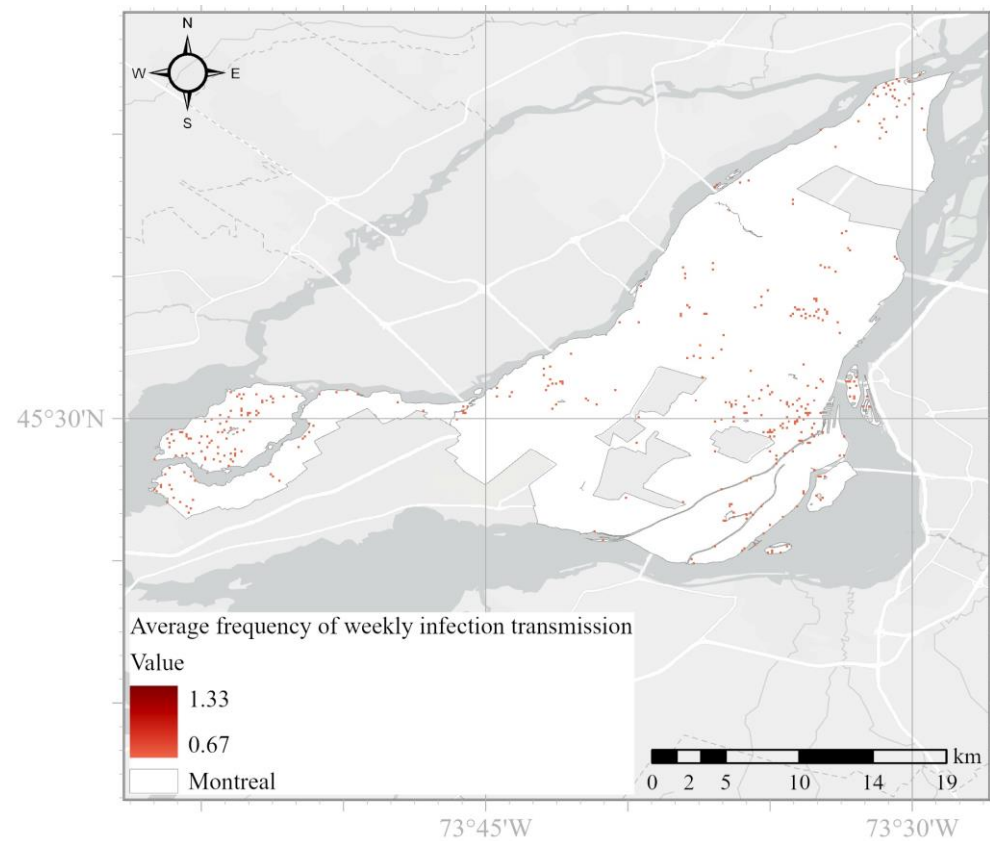


Figure 8. The spatial map of critical locations of COVID-19 spreading in the study area.

3.4. Investigating the Number of Infected Human Agents in Case of Employing COVID-19 Control Interventions

In this study, the efficacy of two control interventions of reduction in human mobility and self-isolation was evaluated. To do so, the control intervention parameters were made configurable in the models so that users could change them dynamically in the simulation. Dynamically defining parameters enabled us to change the configuration and evaluate the efficacy of interventions. In the remainder of this section, the efficacy of two interventions was evaluated.

3.4.1. Reduction in Human-Mobility

To evaluate the impacts of reduction in human mobility on the COVID-19 outbreak, the disease outbreak was assumed in two ways: as it was before the outbreak (i.e., people’s ordinary movement) and as it was during the COVID-19 outbreak (i.e., reduction in people’s movement). Following the COVID-19 community mobility reports (<https://www.google.com/covid19/mobility/>) (accessed on 24 April 2022), the movement of people in the study area to public places and workplaces, respectively, decreased by 33% and 18%, on average, from January to February 2021. The number of newly infected human agents was depicted in Figure 9 in both modes of considering ordinary movement and movement reduction.

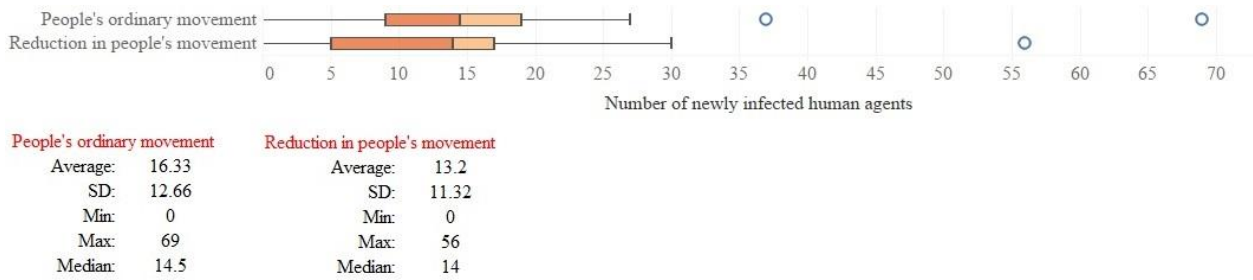


Figure 9. The number of newly infected human agents in two modes of considering people’s ordinary movement as well as a reduction in people’s movement; each agent is a representative of 100 people.

Concerning Figure 9, when individuals follow the rule of reducing people’s mobility, the number of infected people decreases by about 63 a week, on average. In other words, if people had kept following their normal ordinary movement from 5 January to 9 February, the number of infected cases would have risen by around 63 a week, on average.

3.4.2. Self-Isolation Intervention

To assess the self-isolation intervention impact, three distinct values of 10%, 20%, and 30% in addition to the adjusted value (i.e., 42%) were considered as the percentage of infectious people who follow the self-isolation intervention. It is important to mention that these values were defined subjectively and without any specific literature to support it. In Figure 10, the number of newly infected human agents obtained from the model for three values were compared to the results obtained regarding the adjusted value (i.e., 42%) for the self-isolation parameter after the calibration.

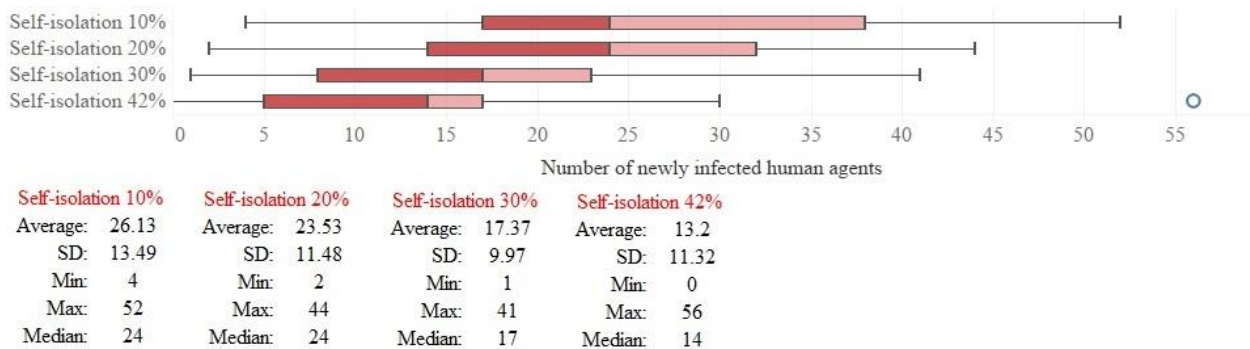


Figure 10. The number of newly infected human agents regarding four distinct values for the percentage of infectious people observing the self-isolation intervention; each agent is a representative of 100 people.

As shown in Figure 10, if instead of 42%, 10%, 20%, and 30% of infectious people had isolated themselves from 5 January to 9 February, the number of infected people would have increased by about 259, 207, and 83 more a week, on average, respectively.

4. Discussion

Disasters like the COVID-19 epidemic might have less ramifications in case of grasping appropriate understandings of issues such as how humans and social systems operate under diverse situations, how individuals and societies adapt to disrupted complex social systems, and what feasible procedures can be performed [51]. Modeling the dynamic outbreak of COVID-19 allow researchers and decision makers to understand these processes. A variety of spatial epidemiological modeling approaches have been developed during the last several decades [52]. The mathematical modeling approach, as one of the epidemiological modeling approaches, has been used in many earlier studies to explain and anticipate epidemics, as well as predict the consequences of public health measures [11,53–57]. When comparing two epidemiological modeling approaches of mathematical and ABM, mathematical models are essentially aggregate-based since they represent overall transition rates in a population among disease states. In addition to homogenous consideration of population in mathematical models, fundamental spatial dynamics such as population mobility and interactions which are crucial for the spread of any infectious disease, particularly COVID-19, have been also largely ignored. In contrast, the ABM approach is individual-based and considers the heterogeneity in modeling. Furthermore, the ABM approach simulates epidemics by considering individuals' movements and interactions given the space. The capabilities of the ABM approach were the driving force behind our decision to apply it in the COVID-19 pandemic simulation.

To curb the COVID-19 outbreak, stringent control measures have been implemented around the world [58]. One of these measures is restrictions on people's mobility and travel [7,22,59]. Even though any movement has the potential to spread disease, internal mobility appears to be more essential than cross-provincial mobility [60]. To assess the efficacy of people's mobility inside of Montreal city, we used spatial data and simulated the movements of people in accordance with the spatial data as well as some attributes of human agents such as age and occupation. Following the reduction in the number of infected people concerning the reduction in humans' mobility, it was concluded that people's movement was a crucial role in the COVID-19 outbreak. Our findings were consistent with the results of several earlier research [22,59–61].

Even though people's willingness to self-isolate is influenced by their socioeconomic status [62], self-isolation could be another important intervention against contagious diseases, particularly COVID-19 [63]. Accordingly, the impact of the self-isolation intervention was explored in addition to the effectiveness of reducing human mobility in this study. Regarding the results of our model, the self-isolation of the infectious population leads to a remarkable drop in the number of infected people. Following our findings and those of other studies [12,64,65], self-isolation of infectious people could lead to drastically reducing the COVID-19 outbreak.

Strengths and limitations

The strengths of our ABM included: (i) providing a comprehensive description of the COVID-19 transmission cycle among a population; (ii) integrating the ABM approach with GIS and using spatial data to model movements and interactions of human agents and construct a spatial epidemic model; (iii) considering multiple places for human agents to move during the day to create a more dynamic model; (iv) defining a various interaction levels approach and exerting it in the computation of COVID19-transmission probability instead of identical considering of human agents' interactions with one another; (v) taking into account various number of daily interactions and employing it in calculating the probability of COVID-19 transmission; (vi) doing model calibration process using the HM method; (vii) validating the model using the Chi-square test; (viii) providing a map depicting the hotspots of COVID-19 as the only spatial data on COVID-19 occurrences available in the study area; and (ix) investigating the efficacy of two hitherto underappreciated control interventions.

Notwithstanding these strengths, this study had certain limitations in terms of model validation. The model was validated regarding the temporal pattern of COVID-19 and

the validation of the model from a spatial perspective was not feasible due to the lack of spatial COVID-19 occurrences data at the city scale. Besides, owing to the computationally intensive nature of agent-based models and the limited memory capacity of computers, not all the population and activities could be considered. Accordingly, each agent was considered as the representative of 100 individuals in the real world. As a result, this widened the gap between the results of the model and reality and consequently affects the validation of the model. This is also another limitation in the validation of agent-based models.

5. Conclusions

COVID-19 has caused high mortality and unprecedented restrictions on social and economic activities throughout the world. This study concentrated on the development of a GIS-based ABM in which the COVID-19 outbreak was assumed among heterogeneous populations so that their exclusive interactions and movements were considered in a spatial-based environment. The principal focus of this research was to: (1) simulate the COVID-19 outbreak progression in the city of Montreal, QC, Canada, by considering the geospatial context of the outbreak; (2) assess the effectiveness of two control interventions on containing the COVID-19 outbreak; (3) provide a map illustrating the spreading hotspots of the COVID-19 in the study area; (4) provide a flexible decision-making platform by designing various user-defined parameters; and (5) track the number of people in various health statuses over time. The ODD protocol was used to explain the model. The calibration of the model was performed using the HM method. In addition, the proposed model was validated regarding the temporal pattern of the COVID-19 outbreak using the Chi-square test. Two crucial control interventions of reduction in human mobility and self-isolation were implemented in the model to provide information about their efficacy in curbing the COVID-19 outbreak in the study area. Our simulation experiments indicated that the mainstream of COVID-19 transmissions (i.e., approximately 90.34%) occurred in public places. Besides, following the derived number of newly infected cases from 5 January to 9 February 2021, it can be inferred that the rules aiming to reduce population mobility, led to a reduction of about 63 infected people each week, on average. Furthermore, our scenarios revealed that if instead of 42% (i.e., the adjusted value in the calibration), 10%, 20%, and 30% of infectious people had followed the self-isolation measure, the number of infected people would have risen by approximately 259, 207, and 83 more each week, on average, respectively. Regarding the findings of this research, it was inferred that both control interventions could remarkably contain the COVID-19 outbreak. In conclusion, the specifics and findings of our GIS-based ABM could pave the way for the government in advising on pandemic decision-making. This research can be the basis for deploying forward-looking controlling interventions in the study area.

Author Contributions: Conceptualization, methodology, validation, formal analysis, investigation, resources, writing—review and editing, Navid Mahdizadeh Gharakhanlou and Liliana Perez; software, data curation, writing—original draft preparation and visualization, Navid Mahdizadeh Gharakhanlou; supervision, project administration and funding acquisition, Liliana Perez. All authors have read and agreed to the published version of the manuscript.

Funding: This research was partially funded by [the Natural Sciences and Engineering Research Council (NSERC) of Canada through the Discovery], Grant number [RGPIN/05396-2016] awarded to L.P. The funders had no role in the study design, data collection, and analysis, decision to publish, or preparation of the manuscript. There was no additional external funding received for this study.

Data Availability Statement: All the required data and code to replicate our findings can be found here: COVID-19_Model.

Acknowledgments: We appreciate the constructive comments received from the three reviewers on an earlier version of the manuscript.

Conflicts of Interest: The authors declare no conflict of interest.

Appendix A

Demographic information of Montreal city as well as its labor statistics.

Table A1. The population of Montreal city based on age (the year 2016).

Age Range	Agent Number (Each Agent Represents 10 People in the Real World)	Population (in 2016)	Percentage (%)
0 to 4 Years	10,991	109,910	5.8%
5 to 9 Years	10,044	100,435	5.3%
10 to 14 Years	8528	85,275	4.5%
15 to 19 Years	9096	90,960	4.8%
20 to 29 Years	29,751	297,515	15.7%
30 to 39 Years	30,699	306,990	16.2%
40 to 49 Years	24,824	248,245	13.1%
50 to 59 Years	24,824	248,245	13.1%
60 to 69 Years	19,329	193,290	10.2%
70 Years and over	21,414	214,135	11.3%
Total	189,500	1,895,000	100%

Table A2. The number of households based on household size (the year 2016).

Household's Size	Number of Households	Population	Population (Based on Agents)	Number of Households (Based on Agent)
1 person	342,510 (39.12%)	342,510	34,251	34,251
2 persons	259,295 (29.62%)	518,590	51,860	25,930
3 persons	118,645 (13.55%)	355,935	35,592	11,864
4 persons	97,490 (11.13%)	389,960	38,996	9749
5 persons and more	57,601(6.58%)	288,005	28,800	5760
Total	875,541	1,895,000	189,499	87,554

Table A3. Labor statistics of people 15 years of age and over in the year 2016 [66].

People	Number (Real World)	Agent Number	Percentage
Employed	Employee	81,096	50.71%
	Self-employed	23,158	14.48%
Unemployed	91,645	9164	5.73%
Students (70% of people with 15–29 years of age)	271,932	27,193	17%
Not determined	193,268	19,327	12.08%
Total population of 15 years and over	1,599,380	159,938	100%

Appendix B

The implementation flowchart of the proposed agent-based model on the Mesa framework.

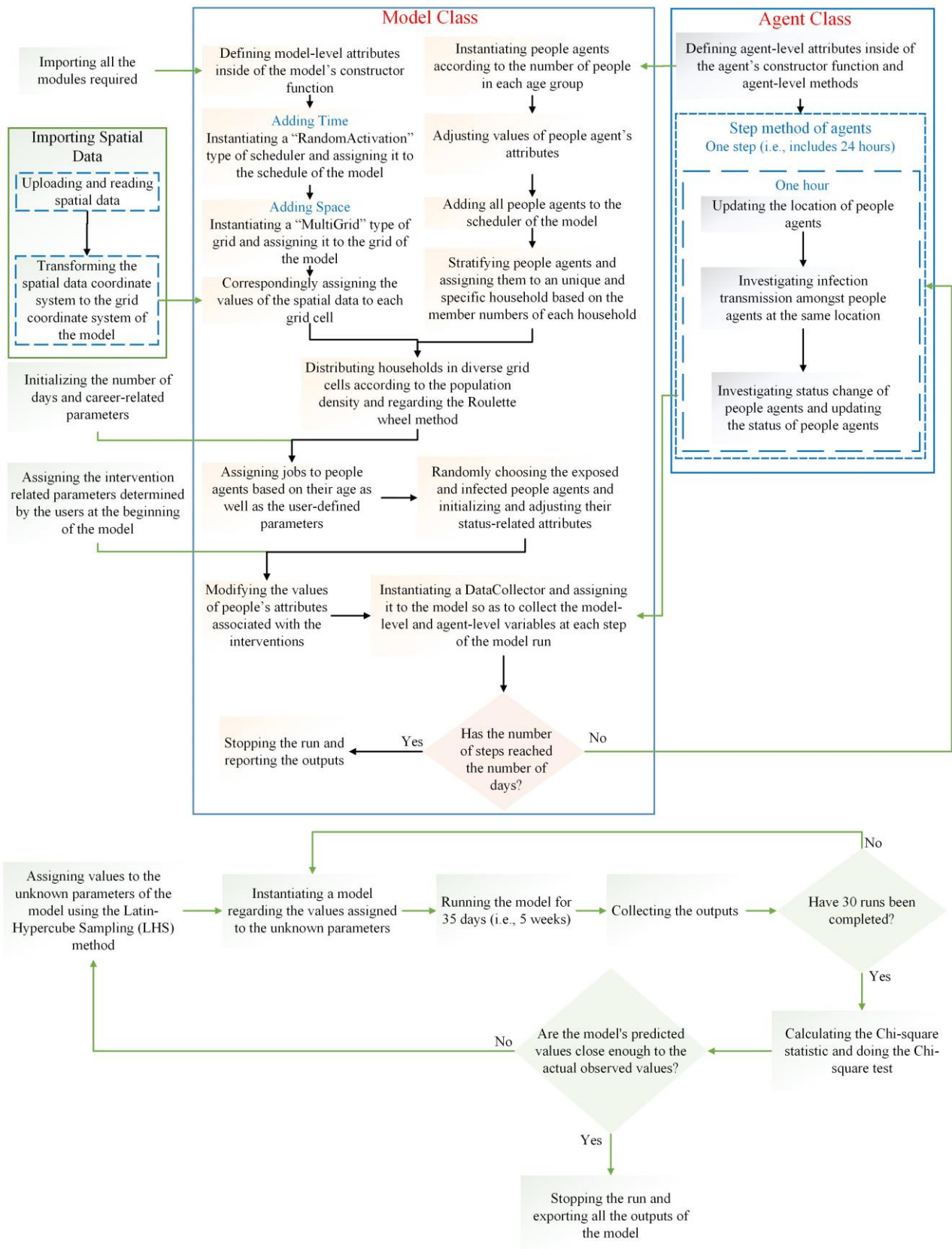


Figure A1. Code implementation processes in Mesa.

Appendix C

All parameters used in calculation of infection-transmission probability.

Table A4. The values of parameters considered in the calculation of the infection-transmission probability.

Parameters	Symbol	Value	Resources
Mean of the infectious period	μ	5.5 days	Ferretti et al., 2020 [67]; Hinch et al., 2021 [36]
The standard deviation of the infectious period	σ	2.14 days	
Mean number of people infected by each infected person	R_0	4.5	Ke et al., 2021 [38]
Infectious rate of asymptomatic individuals relative to severely symptomatic individuals	A_{asym}	0.33	Hinch et al., 2021 [36]
Infectious rate of mildly symptomatic individuals relative to severely symptomatic individuals	A_{mild}	0.72	Hinch et al., 2021 [36]
	S_{0-9}	0.35	
	S_{10-19}	0.69	
	S_{20-29}	1.03	
	S_{30-39}	1.03	
	S_{40-49}	1.03	
	S_{50-59}	1.03	
	S_{60-69}	1.27	
	$S_{70 \text{ and } 70+}$	1.52	
Relative susceptibility of recipient to infection based on age			Zhang et al., 2020 [68]

Appendix D

Daily number of people's interactions.

Table A5. The daily number of interactions of people based on age [44].

Age Range	Daily Number of Interactions, Normal Distribution with Mean (Standard Deviation)
0–4	10.21 (7.65)
5–9	14.81 (10.09)
10–14	18.22 (12.27)
15–19	17.58 (12.03)
20–29	13.57 (10.6)
30–39	14.14 (10.15)
40–49	13.83 (10.86)
50–59	12.30 (10.23)
60–69	9.21 (7.96)
70+	6.89 (5.83)

References

1. Ali, M.; Ahsan, G.U.; Khan, R.; Khan, H.R.; Hossain, A. Immediate impact of stay-at-home orders to control COVID-19 transmission on mental well-being in Bangladeshi adults: Patterns, Explanations, and future directions. *BMC Res. Notes* **2020**, *13*, 494. [[CrossRef](#)] [[PubMed](#)]
2. Chakraborty, I.; Maity, P. COVID-19 outbreak: Migration, effects on society, global environment and prevention. *Sci. Total Environ.* **2020**, *728*, 138882. [[CrossRef](#)] [[PubMed](#)]

3. Valjarević, A.; Milić, M.; Valjarević, D.; Stanojević-Ristić, Z.; Petrović, L.; Milanović, M.; Filipović, D.; Ristanović, B.; Basarin, B.; Lukić, T. Modelling and mapping of the COVID-19 trajectory and pandemic paths at global scale: A geographer's perspective. *Open Geosci.* **2020**, *12*, 1603–1616. [[CrossRef](#)]
4. Andersen, L.M.; Harden, S.R.; Sugg, M.M.; Runkle, J.D.; Lundquist, T.E. Analyzing the spatial determinants of local COVID-19 transmission in the United States. *Sci. Total Environ.* **2021**, *754*, 142396. [[CrossRef](#)] [[PubMed](#)]
5. Zhou, C.; Su, F.; Pei, T.; Zhang, A.; Du, Y.; Luo, B.; Cao, Z.; Wang, J.; Yuan, W.; Zhu, Y. COVID-19: Challenges to GIS with big data. *Geogr. Sustain.* **2020**, *1*, 77–87. [[CrossRef](#)]
6. Sun, F.; Matthews, S.A.; Yang, T.-C.; Hu, M.-H. A spatial analysis of the COVID-19 period prevalence in US counties through June 28, 2020: Where geography matters? *Ann. Epidemiol.* **2020**, *52*, 54–59.e1. [[CrossRef](#)]
7. O'Sullivan, D.; Gahegan, M.; Exeter, D.; Adams, B. Spatially-explicit models for exploring COVID-19 lockdown strategies. *Trans. GIS* **2020**, *24*, 967–1000. [[CrossRef](#)]
8. Gleeson, J.P.; Brendan Murphy, T.; O'Brien, J.D.; Friel, N.; Bargary, N.; O'Sullivan, D.J. Calibrating COVID-19 susceptible-exposed-infected-removed models with time-varying effective contact rates. *Philos. Trans. R. Soc.* **2022**, *380*, 20210120. [[CrossRef](#)]
9. Chan, S. Complex adaptive systems. In *ESD 83 Research Seminar in Engineering Systems*; MIT: Cambridge, MA, USA, 2001; pp. 1–9.
10. Batty, M.; Torrens, P.M. Modelling and prediction in a complex world. *Futures* **2005**, *37*, 745–766. [[CrossRef](#)]
11. Oliveira, J.F.; Jorge, D.C.; Veiga, R.V.; Rodrigues, M.S.; Torquato, M.F.; da Silva, N.B.; Fiaccone, R.L.; Cardim, L.L.; Pereira, F.A.; de Castro, C.P. Mathematical modeling of COVID-19 in 14.8 million individuals in Bahia, Brazil. *Nat. Commun.* **2021**, *12*, 333. [[CrossRef](#)]
12. Ullah, S.; Khan, M.A. Modeling the impact of non-pharmaceutical interventions on the dynamics of novel coronavirus with optimal control analysis with a case study. *Chaos Solitons Fractals* **2020**, *139*, 110075. [[CrossRef](#)]
13. Gharakhanlou, N.M.; Hooshangi, N. Dynamic simulation of fire propagation in forests and rangelands using a GIS-based cellular automata model. *Int. J. Wildland Fire* **2021**, *30*, 652–663. [[CrossRef](#)]
14. Gaudreau, J.; Perez, L.; Drapeau, P. BorealFireSim: A GIS-based cellular automata model of wildfires for the boreal forest of Quebec in a climate change paradigm. *Ecol. Inform.* **2016**, *32*, 12–27. [[CrossRef](#)]
15. Pérez, L.; Dragičević, S.; White, R. Model testing and assessment: Perspectives from a swarm intelligence, agent-based model of forest insect infestations. *Comput. Environ. Urban Syst.* **2013**, *39*, 121–135. [[CrossRef](#)]
16. Perez, L.; Dragicevic, S.; Gaudreau, J. A geospatial agent-based model of the spatial urban dynamics of immigrant population: A study of the island of Montreal, Canada. *PLoS ONE* **2019**, *14*, e0219188. [[CrossRef](#)]
17. Munshi, J.; Roy, I.; Balasubramanian, G. Spatiotemporal dynamics in demography-sensitive disease transmission: COVID-19 spread in NY as a case study. *arXiv* **2020**, arXiv:2005.01001.
18. White, S.H.; Del Rey, A.M.; Sánchez, G.R. Modeling epidemics using cellular automata. *Appl. Math. Comput.* **2007**, *186*, 193–202. [[CrossRef](#)]
19. Gharakhanlou, N.M.; Hooshangi, N.; Helbich, M. A Spatial Agent-Based Model to Assess the Spread of Malaria in Relation to Anti-Malaria Interventions in Southeast Iran. *ISPRS Int. J. Geo-Inf.* **2020**, *9*, 549. [[CrossRef](#)]
20. Perez, L.; Dragicevic, S. An agent-based approach for modeling dynamics of contagious disease spread. *Int. J. Health Geogr.* **2009**, *8*, 50. [[CrossRef](#)]
21. Gharakhanlou, N.M.; Mesgari, M.S.; Hooshangi, N. Developing an agent-based model for simulating the dynamic spread of Plasmodium vivax malaria: A case study of Sarbaz, Iran. *Ecol. Inform.* **2019**, *54*, 101006. [[CrossRef](#)]
22. Gharakhanlou, N.M.; Hooshangi, N. Spatio-temporal simulation of the novel coronavirus (COVID-19) outbreak using the agent-based modeling approach (case study: Urmia, Iran). *Inform. Med. Unlocked* **2020**, *20*, 100403. [[CrossRef](#)] [[PubMed](#)]
23. Makarov, V.L.; Bakhtizin, A.R.; Sushko, E.D.; Ageeva, A.F. COVID-19 Epidemic Modeling—Advantages of an Agent-Based Approach. *Ekonom. Sotsialnye Peremeny* **2020**, *13*, 58–73.
24. Shamil, M.; Farheen, F.; Ibtihaz, N.; Khan, I.M.; Rahman, M.S. An agent-based modeling of COVID-19: Validation, analysis, and recommendations. *Cogn. Comput.* **2021**, 1–12. [[CrossRef](#)] [[PubMed](#)]
25. Kerr, C.C.; Stuart, R.M.; Mistry, D.; Abeysuriya, R.G.; Rosenfeld, K.; Hart, G.R.; Núñez, R.C.; Cohen, J.A.; Selvaraj, P.; Hagedorn, B. Covasim: An agent-based model of COVID-19 dynamics and interventions. *PLoS Comput. Biol.* **2021**, *17*, e1009149. [[CrossRef](#)]
26. Cuevas, E. An agent-based model to evaluate the COVID-19 transmission risks in facilities. *Comput. Biol. Med.* **2020**, *121*, 103827. [[CrossRef](#)]
27. Gaudou, B.; Huynh, N.Q.; Philippon, D.; Brugière, A.; Chapuis, K.; Taillandier, P.; Larmande, P.; Drogoul, A. Comokit: A modeling kit to understand, analyze, and compare the impacts of mitigation policies against the COVID-19 epidemic at the scale of a city. *Front. Public Health* **2020**, *8*, 563247. [[CrossRef](#)]
28. Grignard, A.; Nguyen-Huu, T.; Taillandier, P.; Alonso, L.; Ayoub, N.; Elkatsha, M.; Palomo, G.; Gomez, M.; Siller, M.; Gamboa, M. Using agent-based modelling to understand advantageous behaviours against COVID-19 transmission in the built environment. In *Proceedings of the International Workshop on Multi-Agent Systems and Agent-Based Simulation*, Paris, France, 4–6 July 1998; pp. 86–98.
29. Abrams, S.; Wambua, J.; Santermans, E.; Willem, L.; Kuylens, E.; Coletti, P.; Libin, P.; Faes, C.; Petrof, O.; Herzog, S.A.J.E. Modelling the early phase of the Belgian COVID-19 epidemic using a stochastic compartmental model and studying its implied future trajectories. *Epidemics* **2021**, *35*, 100449. [[CrossRef](#)]

30. Manout, O.; Ciari, F. Assessing the role of daily activities and mobility in the spread of COVID-19 in Montreal with an agent-based approach. *Front. Built Environ.* **2021**, *7*, 654279. [[CrossRef](#)]
31. Kazil, J.; Masad, D.; Crooks, A. Utilizing python for agent-based modeling: The mesa framework. In Proceedings of the International Conference on Social Computing, Behavioral-Cultural Modeling and Prediction and Behavior Representation in Modeling and Simulation, Pittsburgh, PA, USA, 20–22 September 2022; pp. 308–317.
32. Masad, D.; Kazil, J. MESA: An agent-based modeling framework. In Proceedings of the 14th PYTHON in Science Conference, Austin, TX, USA, 11–17 July 2022; pp. 53–60.
33. Grimm, V.; Berger, U.; Bastiansen, F.; Eliassen, S.; Ginot, V.; Giske, J.; Goss-Custard, J.; Grand, T.; Heinz, S.K.; Huse, G. A standard protocol for describing individual-based and agent-based models. *Ecol. Model.* **2006**, *198*, 115–126. [[CrossRef](#)]
34. Grimm, V.; Berger, U.; DeAngelis, D.L.; Polhill, J.G.; Giske, J.; Railsback, S.F. The ODD protocol: A review and first update. *Ecol. Model.* **2010**, *221*, 2760–2768. [[CrossRef](#)]
35. McAloon, C.; Collins, Á.; Hunt, K.; Barber, A.; Byrne, A.W.; Butler, F.; Casey, M.; Griffin, J.; Lane, E.; McEvoy, D. Incubation period of COVID-19: A rapid systematic review and meta-analysis of observational research. *BMJ Open* **2020**, *10*, e039652. [[CrossRef](#)]
36. Hinch, R.; Probert, W.J.; Nurtay, A.; Kendall, M.; Wymant, C.; Hall, M.; Lythgoe, K.; Bulas Cruz, A.; Zhao, L.; Stewart, A.; et al. OpenABM-Covid19—An agent-based model for non-pharmaceutical interventions against COVID-19 including contact tracing. *PLoS Comput. Biol.* **2021**, *17*, e1009146. [[CrossRef](#)]
37. Pellis, L.; Scarabel, F.; Stage, H.B.; Overton, C.E.; Chappell, L.H.; Lythgoe, K.A.; Fearon, E.; Bennett, E.; Curran-Sebastian, J.; Das, R. Challenges in control of COVID-19: Short doubling time and long delay to effect of interventions. *arXiv* **2020**, arXiv:2004.00117. [[CrossRef](#)]
38. Ke, R.; Romero-Severson, E.; Sanche, S.; Hengartner, N. Estimating the reproductive number R0 of SARS-CoV-2 in the United States and eight European countries and implications for vaccination. *J. Theoret. Biol.* **2021**, *517*, 110621. [[CrossRef](#)]
39. Riccardo, F.; Ajelli, M.; Andrianou, X.; Bella, A.; Del Manso, M.; Fabiani, M. Epidemiological characteristics of COVID-19 cases in Italy and estimates of the reproductive numbers one month into the epidemic. *medRxiv* **2020**, *10*, 1560–7917.
40. Yang, X.; Yu, Y.; Xu, J.; Shu, H.; Liu, H.; Wu, Y.; Zhang, L.; Yu, Z.; Fang, M.; Yu, T. Clinical course and outcomes of critically ill patients with SARS-CoV-2 pneumonia in Wuhan, China: A single-centered, retrospective, observational study. *Lancet Respir. Med.* **2020**, *8*, 475–481. [[CrossRef](#)]
41. Kamel Boulos, M.N.; Geraghty, E.M. Geographical tracking and mapping of coronavirus disease COVID-19/severe acute respiratory syndrome coronavirus 2 (SARS-CoV-2) epidemic and associated events around the world: How 21st century GIS technologies are supporting the global fight against outbreaks and epidemics. *Int. J. Health Geogr.* **2020**, *19*, 12.
42. Schmidt, F.; Dröge-Rothaar, A.; Rienow, A. Development of a Web GIS for small-scale detection and analysis of COVID-19 (SARS-CoV-2) cases based on volunteered geographic information for the city of Cologne, Germany, in July/August 2020. *Int. J. Health Geogr.* **2021**, *20*, 24.
43. Shepherd, H.E.; Atherden, F.S.; Chan, H.M.T.; Loveridge, A.; Tatem, A.J. Domestic and international mobility trends in the United Kingdom during the COVID-19 pandemic: An analysis of facebook data. *Int. J. Health Geogr.* **2021**, *20*, 13. [[CrossRef](#)]
44. Mossong, J.; Hens, N.; Jit, M.; Beutels, P.; Auranen, K.; Mikolajczyk, R.; Massari, M.; Salmaso, S.; Tomba, G.S.; Wallinga, J. Social contacts and mixing patterns relevant to the spread of infectious diseases. *PLoS Med.* **2008**, *5*, e74. [[CrossRef](#)]
45. Macal, C.M.; North, M.J. Agent-based modeling and simulation. In Proceedings of the 2009 Winter Simulation Conference (WSC), Austin, TX, USA, 13–16 December 2009; pp. 86–98.
46. Hassan, S.; Arroyo, J.; Galán Ordax, J.M.; Antunes, L.; Pavón Mestras, J. Asking the oracle: Introducing forecasting principles into agent-based modelling. *J. Artif. Soc. Soc. Simul.* **2013**, *16*, 3. [[CrossRef](#)]
47. Purshouse, R.C.; Ally, A.K.; Brennan, A.; Moyo, D.; Norman, P. Evolutionary parameter estimation for a theory of planned behaviour microsimulation of alcohol consumption dynamics in an English birth cohort 2003 to 2010. In Proceedings of the 2014 Annual Conference on Genetic and Evolutionary Computation, Vancouver, BC, Canada, 12–16 July 2014; pp. 1159–1166.
48. McCulloch, J.; Ge, J.; Ward, J.A.; Heppenstall, A.; Polhill, J.G.; Malleson, N. Calibrating Agent-Based Models Using Uncertainty Quantification Methods. *J. Artif. Soc. Soc. Simul.* **2022**, *25*, 100. [[CrossRef](#)]
49. Pukelsheim, F. The three sigma rule. *Am. Stat.* **1994**, *48*, 88–91.
50. Kirkwood, B.R.; Sterne, J.A. *Essential Medical Statistics*; John Wiley & Sons: Piscataway, NJ, USA, 2010.
51. Rifat, S.A.A.; Liu, W. Measuring community disaster resilience in the conterminous coastal United States. *ISPRS Int. J. Geo-Inf.* **2020**, *9*, 469. [[CrossRef](#)]
52. Bian, L. Spatial approaches to modeling dispersion of communicable diseases—a review. *Trans. GIS* **2013**, *17*, 17. [[CrossRef](#)]
53. Gevertz, J.L.; Greene, J.M.; Sanchez-Tapia, C.H.; Sontag, E.D. A novel COVID-19 epidemiological model with explicit susceptible and asymptomatic isolation compartments reveals unexpected consequences of timing social distancing. *J. Theoret. Biol.* **2021**, *510*, 110539. [[CrossRef](#)]
54. Ahn, I.; Heo, S.; Ji, S.; Kim, K.H.; Kim, T.; Lee, E.J.; Park, J.; Sung, K. Investigation of nonlinear epidemiological models for analyzing and controlling the MERS outbreak in Korea. *J. Theoret. Biol.* **2018**, *437*, 17–28. [[CrossRef](#)]
55. Musa, S.S.; Qureshi, S.; Zhao, S.; Yusuf, A.; Mustapha, U.T.; He, D. Mathematical modeling of COVID-19 epidemic with effect of awareness programs. *Infect. Dis. Model.* **2021**, *6*, 448–460. [[CrossRef](#)]
56. Sameni, R. Mathematical modeling of epidemic diseases; A case study of the COVID-19 coronavirus. *arXiv* **2020**, arXiv:2003.11371.

57. Senapati, A.; Rana, S.; Das, T.; Chattopadhyay, J. Impact of intervention on the spread of COVID-19 in India: A model based study. *J. Theoret. Biol.* **2021**, *523*, 110711. [[CrossRef](#)]
58. Khan, M.H.R.; Hossain, A. Machine learning approaches reveal that the number of tests do not matter to the prediction of global confirmed COVID-19 cases. *Front. Artif. Intell.* **2020**, *3*, 90. [[CrossRef](#)]
59. Kraemer, M.U.; Yang, C.-H.; Gutierrez, B.; Wu, C.-H.; Klein, B.; Pigott, D.M.; Group†, O.C.-D.W.; du Plessis, L.; Faria, N.R.; Li, R. The effect of human mobility and control measures on the COVID-19 epidemic in China. *Science* **2020**, *368*, 493–497. [[CrossRef](#)]
60. Iacus, S.M.; Santamaria, C.; Sermi, F.; Spyratos, S.; Tarchi, D.; Vespe, M. Human mobility and COVID-19 initial dynamics. *Nonlinear Dynam.* **2020**, *101*, 1901–1919. [[CrossRef](#)]
61. Lima, L.; Atman, A. Impact of mobility restriction in COVID-19 superspreading events using agent-based model. *PLoS ONE* **2021**, *16*, e0248708. [[CrossRef](#)]
62. Cevik, M.; Baral, S.D.; Crozier, A.; Cassell, J.A. Support for self-isolation is critical in COVID-19 response. *BMJ* **2021**, *372*, 145. [[CrossRef](#)]
63. Jiang, X.; Niu, Y.; Li, X.; Li, L.; Cai, W.; Chen, Y.; Liao, B.; Wang, E. Is a 14-day quarantine period optimal for effectively controlling coronavirus disease 2019 (COVID-19)? *MedRxiv* 2020. [[CrossRef](#)]
64. Van Zandvoort, K.; Jarvis, C.I.; Pearson, C.A.; Davies, N.G.; Ratnayake, R.; Russell, T.W.; Kucharski, A.J.; Jit, M.; Flasche, S.; Eggo, R.M. Response strategies for COVID-19 epidemics in African settings: A mathematical modelling study. *BMC Med.* **2020**, *18*, 19. [[CrossRef](#)]
65. Flaxman, S.; Mishra, S.; Gandy, A.; Unwin, H.J.T.; Mellan, T.A.; Coupland, H.; Whittaker, C.; Zhu, H.; Berah, T.; Eaton, J.W. Estimating the effects of non-pharmaceutical interventions on COVID-19 in Europe. *Nature* **2020**, *584*, 257–261. [[CrossRef](#)]
66. Statistics Canada. *Labour Force Status, Classification of Instructional Programs, Occupation, National Occupational Classification, Statistics Canada, 2016 Census of Population, Statistics Canada Catalogue No. 98-400-X2016259*; Statistics Canada: Ottawa, ON, Canada, 2016.
67. Ferretti, L.; Wymant, C.; Kendall, M.; Zhao, L.; Nurtay, A.; Abeler-Dörner, L.; Parker, M.; Bonsall, D.; Fraser, C. Quantifying SARS-CoV-2 transmission suggests epidemic control with digital contact tracing. *Science* **2020**, *368*, 199. [[CrossRef](#)]
68. Zhang, J.; Litvinova, M.; Liang, Y.; Wang, Y.; Wang, W.; Zhao, S.; Wu, Q.; Merler, S.; Viboud, C.; Vespignani, A. Changes in contact patterns shape the dynamics of the COVID-19 outbreak in China. *Science* **2020**, *368*, 1481–1486. [[CrossRef](#)]